optica

Mid-infrared laser diodes epitaxially grown on on-axis (001) silicon: supplementary material

MARTA RIO CALVO,[§] LAURA MONGE BARTOLOMÉ,[§] MICHAËL BAHRIZ, GUILHEM BOISSIER, LAURENT CERUTTI, JEAN-BAPTISTE RODRIGUEZ AND ERIC TOURNIÉ[*]

IES, University of Montpellier, CNRS, F-34000 Montpellier, France
**Corresponding author: eric.tournie@umontpellier.fr*

[§]These authors participated equally to the work.

Published 26 March 2020

This document provides supplementary information to "Mid-infrared laser diodes epitaxially grown on on-axis (001) silicon," https://doi.org/10.1364/OPTICA.388383.

1. Band structure of the laser heterostructure

We show in Fig. S1 the band structure of the whole laser heterostructure designed to emit at 2.3 µm. Calculations have been performed using the nextnano™ suite [1] and the parameters compiled by Vurgaftman *et al.* [2]. Fig. S2 shows the details of the band structure of the quantum-well used in the active zone. The origin of the energies is the valance band position of HgTe [1].

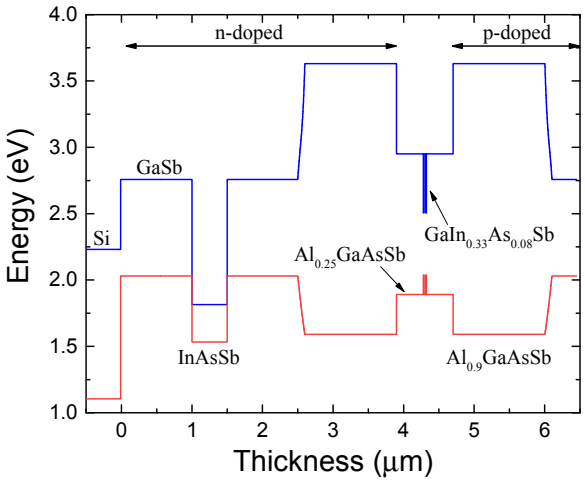

Fig. S1. Overview of the band structure of the whole laser heterostructure.

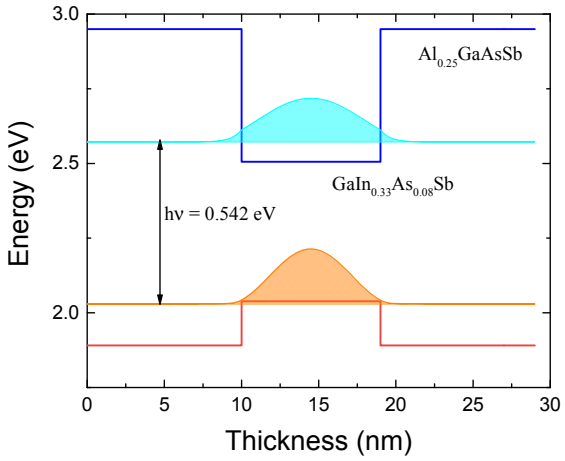

Fig. S2. Band structure of a $Ga_{0.67}In_{0.33}As_{0.08}Sb_{0.92}/Al_{0.25}Ga_{0.75}As_{0.02}Sb_{0.98}$ quantum well used in the active zone, including the representation of the electron (blue-green) and hole (orange) wavefunctions.

2. Anti-phase domains and anti-phase boundaries – Threading dislocation densities

When growing a compound semiconductor, such as a III-V semiconductor, on an on-axis (001) Si substrate, the polarity mismatch between non-polar Si and polar III-V semiconductors easily gives rise to so-called anti-phase domains (APDs) separated by planar defects, the anti-phase boundaries (APBs) [3]. APBs act as shorts in devices and must be avoided to preserve the diode behavior of a semiconductor laser [4].

Atomic force microscopy (AFM) allows imaging the emergence of APBs at the sample surface, as shown in Fig. S3 (a). We show in Fig. S3 (b) a large-scale (20 x 20 μm^2) AFM image of the laser heterostructure investigated in this letter. This figure shows the absence of APBs emerging at the sample surface. This does not mean that there are no APBs at all in the whole structure, but it shows that if any, they do not reach the sample surface. In addition, the well-behaved diode characteristics of the devices indicate that if there are APBs, they are confined below the active region [4]. Finally, the sample exhibits a roughness RMS of ~3.8 nm, a value compatible with laser diode processing.

Preliminary cross-section transmission electron microscopy (TEM) investigations have been carried out on this sample. Three TEM lamellae, each 4-µm wide and 100-nm thick, have been analyzed. This corresponds to 3 x 4 µm x 100 nm = 1.2 $x10^{-8}$ cm^2 of analyzed active-zone interface. No dislocation was found in these lamellae, which gives an upper bound of 8.5 $x10^7$ cm^{-2} for the threading dislocation density (TDD). Still, cross-section TEM is not the best technique to obtain a precise value of TDDs in this range. Detailed investigations will be carried out to precisely assess the sample microstructure and its correlation to the laser performance.

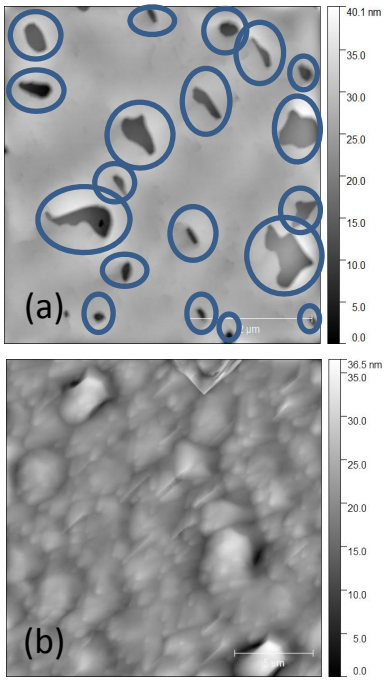

Fig. S3. (a) 5x5 μm^2 AFM picture of a 5006nm thick GaSb epitaxial layer grown on an on-axis (001) Si substrate in conditions which give rise to APDs and APBs. The circles show the APDs. (b) 20x20 μm^2 AFM picture of the laser heterostructure revealing the absence of APDs.

3. Laser diodes with 5 µm and 10 wide ridges

In addition to the 8-µm ridge LDs presented in details in the main text, we have thoroughly characterized series of LDs with 5 µm and 10 µm ridge width. We show the corresponding L – I – V curves taken in cw regime at room temperature and the η_d^{-1} *vs.* L data in Figs. S4 and S5, respectively.

The 5 µm wide ridge LDs exhibit threshold currents between 60 and 125 mA depending on the cavity length (Fig. S4 (a)). The η_d^{-1} *vs.* L data give internal losses around 2 cm^{-1} and an internal quantum efficiency around 35% (Fig. S4 (b)). The threshold current of 10 µm wide ridge LDs vary between 100 and 200 mA depending on the cavity length (Fig. S5 (a)), while the internal losses is estimated around 2 cm^{-1} and the internal quantum efficiency around 32% (Fig. S5 (b)).

Together with the data presented in the main text, these figures confirm the low losses and the high internal quantum efficiency achieved with this laser heterostructure grown on on-axis (001) Si substrate.

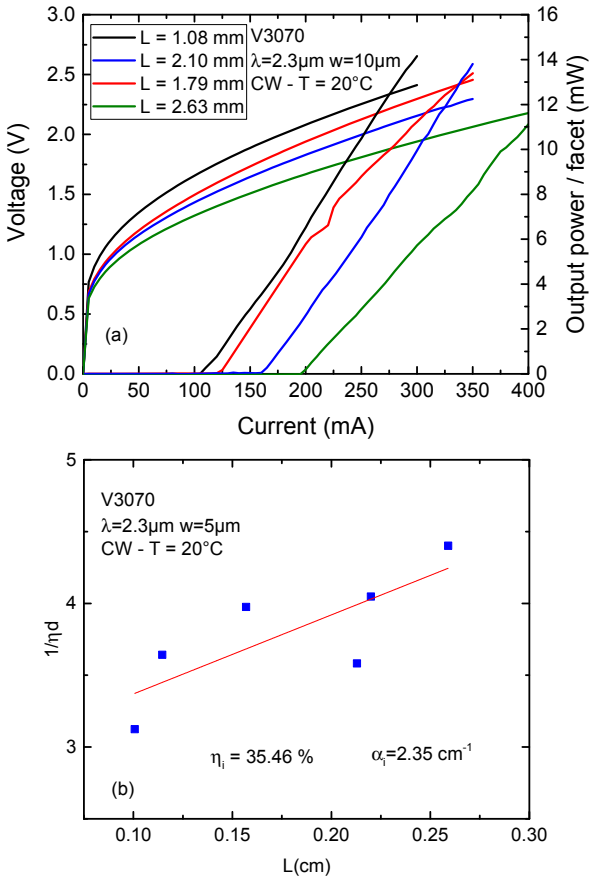

Fig. S4. (a) L – I – V curves taken at 20 °C in cw mode from 5 µm wide ridge LDs and various cavity lenth L. (b) Plot of $1/\eta_d$ (double-facet values) as a function of L for these LDs.

4. Comparison with laser diodes grown on GaSb substrates

The only way to make an absolute and reliable comparison between LDs grown on Si and native GaSb substrates would be to grow laser heterostructures on both substrates in the same growth run. In addition, the LD parameters will depend on their target application. Still, careful analysis of the literature [5-7], shows that good-quality GaInAsSb/AlGaAsSb LDs grown on GaSb substrates and emitting near 2.3 µm consistently exhibit threshold current densities in the 100 – 250 $A.cm^{-2}$, internal losses in the 2 – 6 cm^{-1}, internal quantum efficiencies in the 20 – 70%, T_0 in the 50 –

130 K and T_1 in the 150 – 300 K ranges, depending on the precise heterostructure and device.

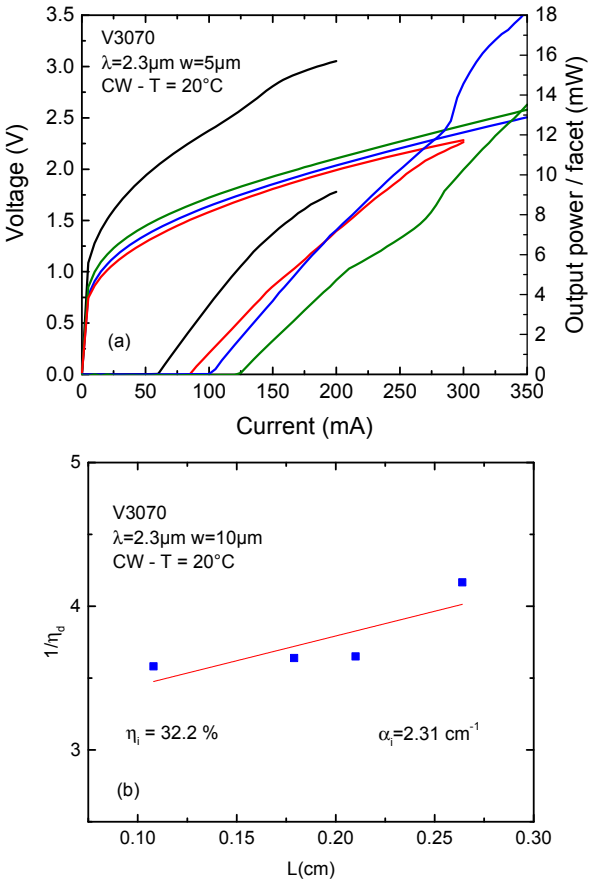

Fig. S5. (a) L – I – V curves taken at 20 °C in cw mode from 10 µm wide ridge LDs and various cavity lenth L. (b) Plot of $1/\eta_d$ (double facet values) as a function of L for these LDs.

References

1. https://www.nextnano.de/
2. I. Vurgaftman, J. R. Meyer, L. R. Ram-Mohan, J. Appl. Phys. **89**, 5815 (2001).
3. H. Kroemer, J. Cryst. Growth **81**, 193 (1987).
4. B. Galiana, I. Rey-Stolle, I. Beinik, C. Algora, C. Teichert, J.M. Molina-Aldareguia, P. Tejedor, Sol. Energy Mater. Sol. Cells **95**, 1949 (2011).
5. G. Belenky, L. Shterengas, M. V. Kisin, T. Hosoda, in "Semiconductor lasers: fundamental and applications", edited by A.N. Baranov and E. Tournié (Woodhead Publishing, Cambridge, 2013) p. 441.
6. L. Cerutti, A. Vicet, A., E. Tournié in "Mid-Infrared optoelectronics: Materials, Devices, Applications", edited by E. Tournié and L. Cerutti (Elsevier, Woodhead Publishing, Duxford, UK, 2019), p. 91.
7. L. Shterengas, G. Kipshidze, T. Hosoda, R. Liang, T. Feng, M. Wang, A. Stein, and G. Belenky, IEEE J. Select. Top. Quant. Electron. **23**, 1500708 (2017).